

Resummed cross section for jet production at hadron colliders

Daniel de Florian

Departamento de Física, FCEYN, Universidad de Buenos Aires, (1428) Pabellón 1 Ciudad Universitaria, Capital Federal, Argentina

Werner Vogelsang

BNL Nuclear Theory, Brookhaven National Laboratory, Upton, New York 11973, USA

(Received 18 April 2007; published 22 October 2007)

We study the resummation of large logarithmic perturbative corrections to the single-inclusive jet cross section at hadron colliders. The corrections we address arise near the threshold for the partonic reaction, when the incoming partons have just enough energy to produce the high-transverse-momentum final state. The structure of the resulting logarithmic corrections is known to depend crucially on the treatment of the invariant mass of the produced jet at threshold. We allow the jet to have a nonvanishing mass at threshold, which most closely corresponds to the situation in experiment. Matching our results to available semianalytical next-to-leading-order calculations, we derive resummed results valid to next-to-leading-logarithmic accuracy. We present numerical results for the resummation effects at Tevatron and RHIC energies.

DOI: [10.1103/PhysRevD.76.074031](https://doi.org/10.1103/PhysRevD.76.074031)

PACS numbers: 12.38.Cy

I. INTRODUCTION

High-transverse-momentum jet production in hadronic collisions, $H_1 H_2 \rightarrow \text{jet } X$, plays a fundamental role in high-energy physics. It offers possibilities to explore QCD, for example, the structure of the interacting hadrons or the emergence of hadronic final states, but is also intimately involved in many signals (and their backgrounds) for new physics. At the heart of all these applications of jet production is our ability to perform reliable and precise perturbative calculations of the partonic short-distance interactions that generate the high-transverse-momentum final states. Up to corrections suppressed by inverse powers of the jet's transverse momentum p_T , the hadronic jet cross section factorizes into parton distribution functions that contain primarily long-distance information, and these short-distance cross sections. In the present paper, we address large logarithmic perturbative corrections to the latter.

At partonic threshold, when the initial partons have just enough energy to produce the high- p_T jet and an unobserved recoiling partonic final state, the phase space available for gluon bremsstrahlung vanishes, so that only soft and collinear emission is allowed, resulting in large logarithmic corrections to the partonic cross section. To be more specific, if we consider the cross section as a function of the jet transverse momentum, integrated over all jet rapidities, the partonic threshold is reached when $\sqrt{s} = 2p_T$, where \sqrt{s} is the partonic center-of-mass (c.m.) energy. Defining $\hat{x}_T \equiv 2p_T/\sqrt{s}$, the leading large contributions near threshold arise as $\alpha_S^k(p_T)\ln^{2m}(1 - \hat{x}_T^2)$ at the k th order in perturbation theory, where $m \leq k$ (the logarithms with $m = k$ are leading) and α_S is the strong coupling. Even if p_T is large so that $\alpha_S(p_T)$ is small, sufficiently close to threshold the logarithmic terms will spoil the

perturbative expansion to any fixed order. Threshold resummation [1–7], however, allows one to reinstate a useful perturbative series by systematically taking into account the terms $\alpha_S^k \ln^{2m}(1 - \hat{x}_T^2)$ to all orders in α_S . This is achieved after taking a Mellin transform of the hadronic cross section in $x_T = 2p_T/\sqrt{s}$, with \sqrt{s} the hadronic c.m. energy. The threshold logarithms exponentiate in transform space.

Regarding phenomenology, the larger x_T , the more dominant will be the threshold logarithms, and hence the more important will be threshold-resummation effects. In addition, because of the convoluted form of the partonic cross sections and the parton distribution functions (PDFs), the steep falloff of the PDFs with momentum fraction x automatically enhances the contributions from the threshold regime to the cross section, because it makes it relatively unlikely that the initial partons have very high c.m. energy. This explains why partonic threshold effects often dominate the hadronic cross section even at not so high x_T . Studies of cross sections for [8] $pp \rightarrow hX$ (with h a high- p_T hadron) and [9–12] $pp \rightarrow \gamma X$ in the fixed-target regime, where typically $0.2 \lesssim x_T \lesssim 0.7$, indeed demonstrate that threshold-resummation effects dominate there and can be very large and important for phenomenology. They enhance the theoretical cross section with respect to fixed-order calculations.

These observations suggest to study the resummation also for jet production at hadron colliders, in particular, when x_T is rather large. An application of particular interest is the jet cross section at very high transverse momenta ($p_T \sim$ several hundreds GeV) at the Tevatron [13,14], for which initially an excess of the experimental data over next-to-leading order (NLO) theory was reported, which was later mostly attributed to an insufficient knowledge of the gluon distribution [15]. Similarly large values of x_T are

now probed in pp collisions at RHIC, where currently $\sqrt{s} = 200$ GeV and jet cross section measurements by the STAR collaboration are already extending to $p_T \gtrsim 40$ GeV [16]. In both of these cases, one does expect threshold-resummation effects to be smaller than in the case of related processes at similar x_T in the fixed-target regime, just because (among other things) the strong coupling constant is smaller at these higher p_T . On the other hand, as we shall see, the effects are still often non-negligible.

Apart from addressing these interesting phenomenological applications, we believe we also improve in this paper the theoretical framework for threshold resummation in jet production. There has been earlier work in the literature on this topic [4,17,18]. In Ref. [4] the threshold-resummation formalism for the closely related dijet production at large invariant mass of the jet pair was developed to next-to-leading logarithmic (NLL) order. In [17], these results were applied to the single-inclusive jet cross section at large transverse momentum, making use of earlier work [6] on the high- p_T prompt-photon cross section, which is kinematically similar. As was emphasized in [4], there is an important subtlety for the resummed jet cross section related to the treatment of the invariant mass of the jet. The structure of the large logarithmic corrections that are addressed by resummation depends on whether or not the jet is assumed to be massless at partonic threshold, even at the leading-logarithmic (LL) level. This is perhaps surprising at first sight, because one might expect the jet mass to be generally inessential since it is typically much smaller than the jet's transverse momentum p_T and in fact vanishes for lowest-order partonic scattering. However, the situation can be qualitatively understood as follows [4]: let us assume that we are defining the jet cross section from the total four-momentum deposited in a cone of aperture R .¹ Considering for simplicity the next-to-leading order, we can have contributions by virtual $2 \rightarrow 2$ diagrams, or by $2 \rightarrow 3$ real-emission diagrams. For the former, a single particle produces the (massless) jet; in case of the latter, there are configurations where two particles in the final state jointly form the jet.

Then, for a jet forced to be massless at partonic threshold, the contributions with two partons in the cone must either have one parton arbitrarily soft, or the two partons exactly collinear. The singularities associated with these configurations cancel against analogous ones in the virtual diagrams, but because the constraint on the real-emission diagrams is so restrictive, large double- and single-logarithmic contributions remain after the cancellation. This will happen regardless of the size R of the cone aperture, implying that the coefficients of the large logarithms will be independent of R . These final-state threshold

logarithms arising from the observed jet suppress the cross section near threshold. Their structure is identical to that of the threshold logarithms generated by the recoiling “jet,” because the latter is not observed and is indeed massless at partonic threshold. The combined final-state logarithms then act against the threshold logarithms associated with initial-state radiation which are positive and enhance the cross section [1].

If, on the other hand, the jet invariant mass is not constrained to vanish near threshold, far more final states contribute—in fact, there will be an integration over the jet mass to an upper limit proportional to the aperture of the jet cone. As the $2 \rightarrow 3$ contributions are therefore much less restricted, the cancellations of infrared and collinear divergences between real and virtual diagrams leave behind only *single* logarithms [4], associated with soft, but not with collinear, emission. Compared to the previously discussed case, there is therefore no double-logarithmic suppression of the cross section by the observed jet, and one expects the calculated cross section to be larger. Also, the single-logarithmic terms will now depend on the jet cone size R .

The resummation for both these cases, with the jet massless or massive at threshold, has been worked out in [4]. The study [17] of the resummed single-inclusive high- p_T jet cross section assumed massless jets at threshold. From a phenomenological point of view, however, we see no reason for demanding the jet to become massless at the partonic threshold. The experimental jet cross sections will, at any given p_T , contain jet events with a large variety of jet invariant masses. NLO calculations of single-inclusive jet cross sections indeed reflect this: they have the property that jets produced at partonic threshold are integrated over a range of jet masses. This becomes evident in the available semianalytical NLO calculations [19–22]. For these, the jet cross section is obtained by assuming that the jet cone is relatively narrow, in which case it is possible to treat the jet definition analytically, so that collinear and infrared final-state divergences may be canceled by hand. This approximation is referred to as the “small-cone approximation (SCA).” Section II.E in the recent calculation in [21] explicitly demonstrates for the SCA that the threshold double logarithms associated with the observed final-state jet cancel, as described above.

In light of this, we will study in this work the resummation in the more realistic case of jets that are massive at threshold. We will in fact make use of the NLO calculation in the SCA approximation of [21] to “match” our resummed cross sections to finite (next-to-leading) order. Knowledge of analytical NLO expressions allows one to extract certain hard-scattering coefficients that are finite at threshold and part of the full resummation formula. These coefficients will be presented and used in our paper for the first time.

We emphasize that the use of the SCA in our work is not to be regarded as a limitation to the usefulness of our

¹Details of the jet definition do not matter for the present argument.

results. First, the SCA is known to be very accurate numerically even at relatively large jet cone sizes of $R \sim 0.7$ [20,21,23]. In addition, one may use our results to obtain ratios of the resummed over the NLO cross sections. Such “ K -factors” are then expected to be extremely good approximations for the effects of higher orders even when one goes away from the SCA and uses, for example, a full NLO Monte Carlo integration code that allows one to compute the jet cross section for larger cone aperture and for other jet definitions (see, for example, Ref. [24]). We will therefore, in particular, present K -factors for the resummed jet cross section in this paper.

The paper is organized as follows: in Sec. II we provide the basic formulas for the single-inclusive jet cross section at fixed order in perturbation theory, and discuss the SCA and the role of the threshold region. Section III presents details of the threshold resummation for the inclusive jet cross section and describes the matching to the analytical expressions for the NLO cross section in the SCA. In Sec. IV we give phenomenological results for the Tevatron and for RHIC. Finally, we summarize our results in Sec. V. The Appendix collects the formulas for the hard-scattering coefficients in the threshold-resummed cross section mentioned above.

II. NEXT-TO-LEADING ORDER SINGLE-INCLUSIVE JET CROSS SECTION

Jets produced in high-energy hadronic scattering, $H_1(P_1)H_2(P_2) \rightarrow \text{jet}(P_J)X$, are typically defined in terms of a deposition of transverse energy or four-momentum in a cone of aperture R in pseudorapidity and azimuthal-angle space, with detailed algorithms specifying the jet kinematic variables in terms of those of the observed hadron momenta [13,25–29]. QCD factorization theorems allow one to write the cross section for single-inclusive jet production in hadronic collisions in terms of convolutions of parton distribution functions with partonic hard-scattering functions [30]:

$$d\sigma = \sum_{a,b} \int dx_1 dx_2 f_{a/H_1}(x_1, \mu_F^2) f_{b/H_2}(x_2, \mu_F^2) d\hat{\sigma}_{ab} \times (x_1 P_1, x_2 P_2, P_J, \mu_F, \mu_R), \quad (1)$$

where the sum runs over all initial partons, quarks, anti-quarks, and gluons, and where μ_F and μ_R denote the factorization and renormalization scales, respectively. It is possible to use perturbation theory to describe the formation of a high- p_T jet, as long as the definition of the jet is infrared safe. The jet is then constructed from a subset of the final-state partons in the short-distance reaction $ab \rightarrow$ partons, and a “measurement function” in the $d\hat{\sigma}_{ab}$ specifies the momentum P_J of the jet in terms of the momenta of the final-state partons, in accordance with the (experimental) jet definition.

The computation of jet cross sections beyond the lowest order in perturbative QCD is rather complicated, due to the need for incorporating a jet definition and the ensuing complexity of the phase space, and due to the large number of infrared singularities of soft and collinear origin at intermediate stages of the calculation. Different methods have been introduced that allow the calculation to be performed largely numerically by Monte Carlo “parton generators,” with only the divergent terms treated in part analytically (see, for example, Ref. [24]).

A major simplification occurs if one assumes that the jet cone is rather narrow, a limit known as the “small-cone approximation (SCA)” [19–22]. In this case, a semianalytical computation of the NLO single-inclusive jet cross section can be performed, meaning that fully analytical expressions for the partonic hard-scattering functions $d\hat{\sigma}_{ab}$ can be derived which only need to be integrated numerically against the parton distribution functions as shown in Eq. (1). The SCA may be viewed as an expansion of the partonic cross section for small $\delta \equiv R/\cosh\eta$, where η is the jet’s pseudorapidity. Technically, the parameter δ is the half-aperture of a geometrical cone around the jet axis, when the four-momentum of the jet is defined as simply the sum of the four-momenta of all the partons inside the cone [19,21]. At small δ , the behavior of the jet cross section is of the form $\mathcal{A} \log(\delta) + \mathcal{B} + \mathcal{O}(\delta^2)$, with both \mathcal{A} and \mathcal{B} known from Refs. [19,21]. Jet codes based on the SCA have the virtue that they produce numerically stable results on much shorter time scales than Monte Carlo codes. Moreover, as we shall see below, the relatively simple and explicit results for the NLO single-inclusive jet cross section obtained in the SCA are a great convenience for the implementation of threshold resummation, particularly for the matching needed to achieve full NLL accuracy.

It turns out that the SCA is a very good approximation even for relatively large cone sizes of up to $R \approx 0.7$ [20,21,23], the value used by both Tevatron collaborations. Figure 1 shows comparisons between the NLO cross sections for single-inclusive jet production obtained using a full Monte Carlo code [24] and the SCA code of [21], for $p\bar{p}$ collisions at c.m. energy $\sqrt{s} = 1800$ GeV and very high p_T . Throughout this paper we use the CTEQ6M [31] NLO parton distribution functions. We have chosen two different jet definitions in the Monte Carlo calculation. One uses a conventional cone algorithm [25], the other the CDF jet definition [13]. One can see that the differences with respect to the SCA are of the order of only a few percent. We note that similar comparisons in the RHIC kinematic regime have been shown in [21]. In their recent paper [16], the STAR collaboration used $R = 0.4$, for which the SCA is even more accurate.

Encouraged by this good agreement, we will directly use the SCA analytical results when performing the threshold resummation. As stated in the Introduction, this is anyway not a limitation, because we will also always provide the

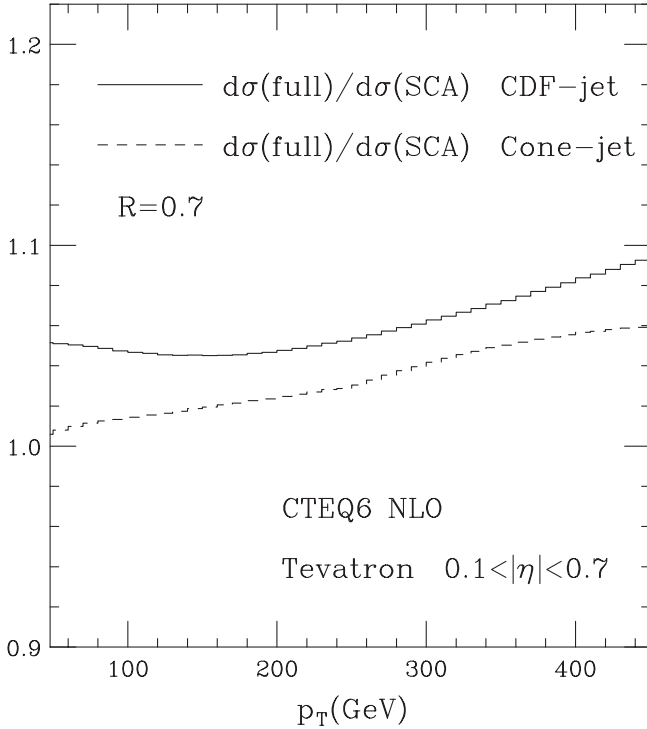


FIG. 1. Ratio between NLO jet cross sections at $\sqrt{s} = 1800$ GeV, computed with a full Monte Carlo code [24] and in the SCA. The solid line corresponds to the jet definition implemented by CDF [13] (with parameter $R_{\text{sep}} = 1.3$), and the dashed one to the standard cone definition [25]. In both cases, the size of the jet cone is set to $R = 0.7$, and the CTEQ6M NLO [31] parton distributions, evaluated at the factorization scale $\mu_F = P_T$, were used.

ratio of resummed over NLO cross sections (K -factors), which may then be used along with full NLO Monte Carlo calculations to obtain resummed cross sections for any desired cone size or jet algorithm.

A further simplification that we will make is to consider the cross section integrated over all pseudorapidities of the jet. As was discussed in [8], this considerably reduces the complexity of the resummed expressions. By simply rescaling the resummed prediction by an appropriate ratio of NLO cross sections, one can nonetheless obtain a very good approximation also for the resummation effects on the nonintegrated cross section, at central rapidities [11]. To perform the NLL threshold resummation for the full rapidity dependence of the jet cross section remains an outstanding task for future work.

From Eq. (1), we find for the single-inclusive jet cross section integrated over all jet pseudorapidity η , in the SCA:²

²We neglect the invariant mass of the jet whenever it is inessential, in particular, in kinematical quantities.

$$\begin{aligned} \frac{p_T^3 d\sigma^{\text{SCA}}(x_T)}{dp_T} &= \sum_{a,b} \int_0^1 dx_1 f_{a/H_1}(x_1, \mu_F^2) \\ &\times \int_0^1 dx_2 f_{b/H_2}(x_2, \mu_F^2) \\ &\times \int_0^1 d\hat{x}_T \delta\left(\hat{x}_T - \frac{x_T}{\sqrt{x_1 x_2}}\right) \\ &\times \int_{\hat{\eta}_-}^{\hat{\eta}_+} d\hat{\eta} \frac{\hat{x}_T^4}{2} \frac{d\hat{\sigma}_{ab}(\hat{x}_T^2, \hat{\eta}, R)}{d\hat{x}_T^2 d\hat{\eta}}, \quad (2) \end{aligned}$$

where as before $x_T \equiv 2p_T/\sqrt{s}$ is the customary scaling variable, and $\hat{x}_T \equiv 2p_T/\sqrt{s}$ with $s = x_1 x_2 S$ is its partonic counterpart. $\hat{\eta}$ is the partonic pseudorapidity, $\hat{\eta} = \eta - \frac{1}{2} \ln(x_1/x_2)$, which has the limits $\hat{\eta}_+ = -\hat{\eta}_- = \ln[(1 + \sqrt{1 - \hat{x}_T^2})/\hat{x}_T]$. The dependence of the partonic cross sections on μ_F and μ_R has been suppressed for simplicity. The perturbative expansion of the $d\hat{\sigma}_{ab}$ in the coupling constant $\alpha_S(\mu_R)$ reads

$$\begin{aligned} d\hat{\sigma}_{ab}(\hat{x}_T^2, \hat{\eta}, R) &= \alpha_S^2(\mu_R) [d\hat{\sigma}_{ab}^{(0)}(\hat{x}_T^2, \hat{\eta}) \\ &+ \alpha_S(\mu_R) d\hat{\sigma}_{ab}^{(1)}(\hat{x}_T^2, \hat{\eta}, R) + \mathcal{O}(\alpha_S^2)]. \quad (3) \end{aligned}$$

As indicated, the leading-order (LO) term $d\hat{\sigma}_{ab}$ has no dependence on the cone size R , because for this term a single parton produces the jet. The analytical expressions for the NLO terms $d\hat{\sigma}_{ab}^{(1)}$ have been obtained in [19,21]. It is customary to express them in terms of a different set of variables, v and w , that are related to \hat{x}_T and $\hat{\eta}$ by

$$\hat{x}_T^2 = 4vw(1-v), \quad e^{2\hat{\eta}} = \frac{vw}{1-v}. \quad (4)$$

Schematically, the NLO corrections to the partonic cross section for each scattering channel then take the form

$$\begin{aligned} \frac{sd\hat{\sigma}_{ab}^{(1)}(w, v, R)}{dw dv} &= A_{ab}(v, R) \delta(1-w) \\ &+ B_{ab}(v, R) \left(\frac{\ln(1-w)}{1-w} \right)_+ \\ &+ C_{ab}(v, R) \left(\frac{1}{1-w} \right)_+ + F_{ab}(w, v, R), \quad (5) \end{aligned}$$

where the “plus” distributions are defined as usual by

$$\int_0^1 dw f(w) [g(w)]_+ \equiv \int_0^1 dw (f(w) - f(1)) g(w), \quad (6)$$

and where the $F_{ab}(w, v, \delta)$ collect all terms without distributions in w . The partonic threshold corresponds to the limit $w \rightarrow 1$. The plus-distribution terms in Eq. (5) generate the large logarithmic corrections that are addressed by threshold resummation. At order k of perturbation theory, the leading contributions are proportional to

$\alpha_S^k \frac{(\ln(1-w))^{2k-1}}{1-w} +$. Performing the integration of these terms over $\hat{\eta}$, they turn into contributions $\propto \alpha_S^k \ln^{2k}(1 - \hat{x}_T^2)$, as we anticipated in the Introduction, and as we shall show below. Subleading terms are down by one or more powers of the logarithm. We will now turn to the NLL resummation of the threshold logarithms.

III. RESUMMED CROSS SECTION

The resummation of the soft-gluon contributions is carried out in Mellin- N moment space, where they exponentiate [1–7]. At the same time, in moment space the convolutions between the parton distributions and the partonic subprocess cross sections turn into ordinary products. For our present calculation, the appropriate Mellin moments are in the scaling variable x_T :³

$$\sigma(N) \equiv \int_0^1 dx_T^2 (x_T^2)^{(N-1)} \frac{p_T^3 d\sigma(x_T)}{dp_T}. \quad (7)$$

In Mellin- N space the QCD factorization formula in Eq. (2) becomes

$$\sigma(N) = \sum_{a,b} f_{a/H}^{N+1}(\mu_F^2) f_{b/H}^{N+1}(\mu_F^2) \hat{\sigma}_{ab}(N), \quad (8)$$

where the $f_{a/H}^N$ are the moments of the parton distribution functions,

$$f_{a/H}^N(\mu_F^2) \equiv \int_0^1 dx x^{N-1} f_{a/H}(x, \mu_F^2), \quad (9)$$

and where

$$\hat{\sigma}_{ab}(N) \equiv \frac{1}{2} \int_0^1 dw \int_0^1 dv [4v(1-v)w]^{N+1} \times \frac{sd\hat{\sigma}_{ab}(w, v)}{dw dv}. \quad (10)$$

The threshold limit $w \rightarrow 1$ corresponds to $N \rightarrow \infty$, and the LL soft-gluon corrections contribute as $\alpha_S^m \ln^{2m} N$. The large- N behavior of the NLO partonic cross sections can be easily obtained by using

$$\int_0^1 [4v(1-v)]^{N+1} f(v) = \int_0^1 [4v(1-v)]^{N+1} \times \left(f\left(\frac{1}{2}\right) + \mathcal{O}\left(\frac{1}{N}\right) \right). \quad (11)$$

Up to corrections suppressed by $1/N$, it is therefore possible to perform the v -integration of the partonic cross sections by simply evaluating them at $v = 1/2$. According to Eq. (5), when $v = 1/2$ is combined with the threshold limit $w = 1$, one has $\hat{x}_T = 1$. It is worth mentioning that in the same limit one has $\hat{\eta} = 0$, and therefore the coefficients for the soft-gluon resummation for the rapidity-integrated cross section agree with those

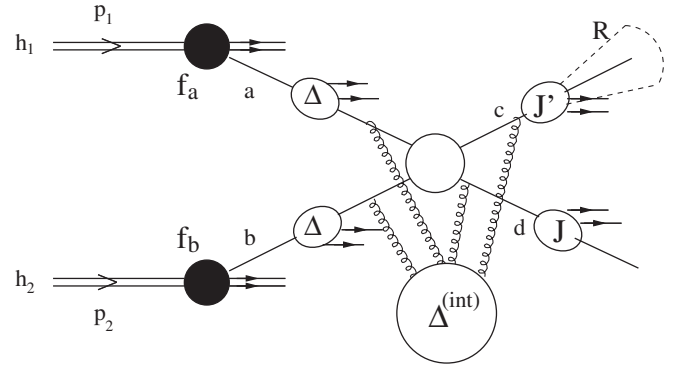


FIG. 2. Pictorial representation of the resummation formula in Eq. (12).

for the cross section at vanishing partonic rapidity. This explains why generally the resummation for the rapidity-integrated hadronic cross section yields a good approximation to the resummation of the cross section integrated over only a finite rapidity interval, as long as a region around $\eta = 0$ is contained in that interval [11].

The resummation of the large logarithms in the partonic cross sections is achieved by showing that they exponentiate in Sudakov form factors. The resummed cross section for each partonic subprocess is given by a formally rather simple expression in Mellin- N space:

$$\hat{\sigma}_{ab}^{(\text{res})}(N) = \sum_{c,d} C_{ab} \Delta_N^a \Delta_N^b J_N^c J_N^d \times \left[\sum_I G_{ab \rightarrow cd}^I \Delta_{IN}^{(\text{int})ab \rightarrow cd} \right] \hat{\sigma}_{ab \rightarrow cd}^{(\text{Bom})}(N), \quad (12)$$

where the first sum runs over all possible final-state partons c and d , and the second over all possible color configurations I of the hard scattering. Except for the Born cross sections $\hat{\sigma}_{ab \rightarrow cd}^{(\text{Bom})}$ (which we have presented in earlier work [8]), each of the N -dependent factors in Eq. (12) is an exponential containing logarithms in N . The coefficients C_{ab} collect all N -independent contributions, which partly arise from hard virtual corrections and can be extracted from comparison to the analytical expressions for the full NLO corrections in the SCA. Finally, the $G_{ab \rightarrow cd}^I$ are color weights obeying $\sum_I G_{ab \rightarrow cd}^I = 1$. The color interferences expressed by the sum over I appear whenever the number of partons involved in the process at Born level is larger than 3, as it is the case here.⁴ Figure 2 gives a simple graphical mnemonic of the structure of the resummation formula, and of the origin of its various factors, whose expressions we now present.

Effects of soft-gluon radiation collinear to the *initial-state* partons are exponentiated in the functions $\Delta_N^{a,b}$, which

³We drop the superscript “SCA” from now on.

⁴In a more general case without rapidity integration, the terms $G_{ab \rightarrow cd}^I \times \hat{\sigma}_{ab \rightarrow cd}^{(\text{Bom})}(N)$ should be replaced by the color-correlated Born cross sections $\hat{\sigma}_{ab \rightarrow cd}^{(\text{Bom}I)}(N)$ [4,7,17].

read

$$\ln \Delta_N^a = \int_0^1 dz \frac{z^{N-1} - 1}{1-z} \int_{\mu_F^2}^{(1-z)^2 Q^2} \frac{dq^2}{q^2} A_a(\alpha_S(q^2)), \quad (13)$$

(and likewise for b) where $Q^2 = 2p_T^2$. J_N^d is the exponent associated with collinear, both soft and hard, radiation in the unobserved recoiling jet,

$$\begin{aligned} \ln J_N^d = & \int_0^1 dz \frac{z^{N-1} - 1}{1-z} \left[\int_{(1-z)^2 Q^2}^{dq^2} \frac{dq^2}{q^2} A_d(\alpha_S(q^2)) \right. \\ & \left. + \frac{1}{2} B_d(\alpha_S((1-z)Q^2)) \right]. \end{aligned} \quad (14)$$

The function J_N^c describes radiation in the observed jet. As we reviewed in the Introduction, this function is sensitive to the assumption made about the jet's invariant mass at threshold [4] even at LL level. Our choice is to allow the jet to be massive at partonic threshold, which is consistent with the experimental definitions of jet cross sections and with the available NLO calculations. In this case, J_N^c is given as

$$\begin{aligned} \ln J_N^c = & \int_0^1 dz \frac{z^{N-1} - 1}{1-z} C'_c(\alpha_S((1-z)^2 Q^2)) \\ & \text{(jet massive at threshold)}. \end{aligned} \quad (15)$$

A similar exponent was derived for this case in [4]. The expression given in Eq. (15) agrees with the one of [4] to the required NLL accuracy. Notice that J_N^c contains only single logarithms, which arise from soft emission, whereas logarithms of collinear origin are absent. This is explicitly seen in the NLO calculations in the SCA [20,21] in which there is an integration over the jet mass up to a maximum value of $\mathcal{O}(\delta \sim R)$, even when the threshold limit is strictly reached. Collinear contributions that would usually generate large logarithms are actually “regularized” by the cone size δ and give instead rise to $\log(\delta)$ terms in the perturbative cross sections.

If, however, the jet is forced to be massless at partonic threshold, the jet function is identical to the function for an “unobserved” jet given in Eq. (14) [4,17]:

$$\ln J_N^c = \ln J_N^c \quad \text{(jet massless at threshold)}, \quad (16)$$

which produces a (negative) double logarithm per emitted gluon, because it also receives collinear contributions due to the stronger restriction on the gluon phase space. There is then no dependence on $\log(\delta)$ in this case.

Finally, large-angle soft-gluon emission is accounted for by the factor $\Delta_{IN}^{(int)ab \rightarrow cd}$, which reads

$$\ln \Delta_{IN}^{(int)ab \rightarrow cd} = \int_0^1 dz \frac{z^{N-1} - 1}{1-z} D_{Iab \rightarrow cd}(\alpha_S((1-z)^2 Q^2)), \quad (17)$$

and depends on the color configuration I of the participating partons.

The coefficients $A_a, B_a, C'_a, D_{Iab \rightarrow cd}$ in Eqs. (13)–(15) and (17) are free of large logarithmic contributions and are given as perturbative series in the coupling constant α_S :

$$\mathcal{F}(\alpha_S) = \frac{\alpha_S}{\pi} \mathcal{F}^{(1)} + \left(\frac{\alpha_S}{\pi}\right)^2 \mathcal{F}^{(2)} + \dots \quad (18)$$

for each of them. For the resummation to NLL accuracy we need the coefficients $A_a^{(1)}, A_a^{(2)}, B_a^{(1)}, C'_a^{(1)}$, and $D_{Iab \rightarrow cd}^{(1)}$. The last of these depends on the specifics of the partonic process under consideration; all the others are universal in the sense that they only distinguish whether the parton they are associated with is a quark or a gluon. The LL and NLL coefficients $A_a^{(1)}, A_a^{(2)}$, and $B_a^{(1)}$ are well known [32]:

$$A^{(1)} = C_a, \quad A^{(2)} = \frac{1}{2} C_a K, \quad B_a^{(1)} = \gamma_a \quad (19)$$

with

$$K = C_A \left(\frac{67}{18} - \frac{\pi^2}{6} \right) - \frac{5}{9} N_f, \quad (20)$$

where $C_g = C_A = N_c = 3$, $C_q = C_F = (N_c^2 - 1)/2N_c = 4/3$, $\gamma_q = -3/2C_F = -2$, $\gamma_g = -2\pi b_0$, and N_f is the number of flavors. The coefficients $C'_a^{(1)}$ needed in the case of jets that are massive at threshold may be obtained by comparing the first-order expansion of the resummed formula to the analytic NLO results in the SCA. They are also universal and read

$$C'_a^{(1)} = -C_a \log\left(\frac{\delta^2}{8}\right). \quad (21)$$

This coefficient contains the anticipated dependence on $\log(\delta)$ that regularizes the final-state collinear configurations. As expected from a term of collinear origin, the exponent (15) hence provides one power of $\log(\delta)$ for each perturbative order.

The coefficients $D_{Iab \rightarrow cd}^{(1)}$ governing the exponentiation of large-angle soft-gluon emission to NLL accuracy, and the corresponding “color weights” $G_{Iab \rightarrow cd}$, depend both on the partonic process and on its “color configuration.” They can be obtained from [4,5,17,33,34] where the soft anomalous dimension matrices were computed for all partonic processes. The results are given for the general case of arbitrary partonic rapidity $\hat{\eta}$. As discussed above, the coefficients for the rapidity-integrated cross section may be obtained by setting $\hat{\eta} = 0$. We have presented the full set of the $D_{Iab \rightarrow cd}^{(1)}$ and $G_{Iab \rightarrow cd}$ in the Appendix of our previous paper [8].

Before we continue, we mention that one expects that a jet cross section defined by a cone algorithm will also have so-called “nonglobal” threshold logarithms [35,36]. These logarithms arise when the observable is sensitive to radiation in only a limited part of phase space, as is the case in the presence of a jet cone. For instance, a soft gluon radiated at an angle *outside* the jet cone may itself emit a secondary gluon at large angle that happens to fall *inside*

the jet cone, thereby becoming part of the jet [35,36]. Such configurations appear first at the next-to-next-to-leading order (NNLO), but may produce threshold logarithms at the NLL level. If the nonglobal logarithms are not suppressed by the cone-opening R in the SCA, our NLL resummation formulas given above will not be complete. In the present paper, we do not take into account threshold corrections associated with the nonglobal logarithms but leave these to a future study. We stress again that any extra contributions from nonglobal logarithms can only start at the NNLO level and will therefore presumably be less important than the “global” threshold terms we include.

Returning to our resummed formulas, it is instructive to consider the structure of the leading logarithms. The LL expressions for the radiative factors are

$$\begin{aligned}\Delta_N^a &= \exp\left[\frac{\alpha_S}{\pi} C_a \ln^2(N)\right], \\ J_N^d &= \exp\left[-\frac{\alpha_S}{2\pi} C_d \ln^2(N)\right].\end{aligned}\quad (22)$$

As discussed above, J^c does not contribute at the double-logarithmic level. Therefore, for a given partonic channel, the leading logarithms are

$$\hat{\sigma}_{ab\rightarrow cd}^{(\text{res})}(N) \propto \exp\left[\frac{\alpha_S}{\pi} \left(C_a + C_b - \frac{1}{2}C_d\right) \ln^2(N)\right]. \quad (23)$$

The exponent is positive for each partonic channel, implying that the soft-gluon effects will increase the cross section. This enhancement arises from the initial-state radiation represented by the $\Delta_{a,b}$ and is related to the fact that finite partonic cross sections are obtained after collinear (mass) factorization [1,2]. In the $\overline{\text{MS}}$ scheme such an enhancing contribution is (for a given parton species) twice as large as the suppressing one associated with final-state radiation in J^d , for which no mass factorization is needed. For quark or antiquark initiated processes, the color factor combination appearing in Eq. (23) ranges from $2C_F - C_F/2 = 2$ for the $qq \rightarrow qq$ channel to $2C_F - C_A/2 = 7/6$ for $q\bar{q} \rightarrow gg$, while for those involving a quark-gluon initial state one has larger factors, $C_F + C_A - C_F/2 = 11/3$ (for $qg \rightarrow qg$) or $C_F + C_A - C_A/2 = 17/6$ (for $qg \rightarrow gq$). Yet larger factors are obtained for gluon-gluon scattering, with $2C_A - C_A/2 = 9/2$ for $gg \rightarrow gg$ and $2C_A - C_F/2 = 16/3$ for $gg \rightarrow q\bar{q}$. Initial states with more gluons therefore are expected to receive the larger resummation effects. We mention that, if the observed jet is assumed strictly massless at threshold, an extra suppression term proportional to J^c arises [see Eq. (16)].

It is customary to give the NLL expansions of the Sudakov exponents in the following way [2]:

$$\ln \Delta_N^a(\alpha_S(\mu_R^2), Q^2/\mu_R^2; Q^2/\mu_F^2) = \ln N h_a^{(1)}(\lambda) + h_a^{(2)}(\lambda, Q^2/\mu_R^2; Q^2/\mu_F^2) + \mathcal{O}(\alpha_S(\alpha_S \ln N)^k), \quad (24)$$

$$\ln J_N^a(\alpha_S(\mu_R^2), Q^2/\mu_R^2) = \ln N f_a^{(1)}(\lambda) + f_a^{(2)}(\lambda, Q^2/\mu_R^2) + \mathcal{O}(\alpha_S(\alpha_S \ln N)^k), \quad (25)$$

$$\ln J_N^a(\alpha_S(\mu_R^2)) = \frac{C_a^{(1)}}{2\pi b_0} \ln(1-2\lambda) + \mathcal{O}(\alpha_S(\alpha_S \ln N)^k), \quad (26)$$

$$\ln \Delta_{IN}^{(\text{in})ab\rightarrow cd}(\alpha_S(\mu_R^2)) = \frac{D_{ab\rightarrow cd}^{(1)}}{2\pi b_0} \ln(1-2\lambda) + \mathcal{O}(\alpha_S(\alpha_S \ln N)^k), \quad (27)$$

with $\lambda = b_0 \alpha_S(\mu_R^2) \ln N$. The LL and NLL auxiliary functions $h_a^{(1,2)}$ and $f_a^{(1,2)}$ are

$$h_a^{(1)}(\lambda) = + \frac{A_a^{(1)}}{2\pi b_0 \lambda} [2\lambda + (1-2\lambda) \ln(1-2\lambda)], \quad (28)$$

$$\begin{aligned}h_a^{(2)}(\lambda, Q^2/\mu_R^2; Q^2/\mu_F^2) &= -\frac{A_a^{(2)}}{2\pi^2 b_0^2} [2\lambda + \ln(1-2\lambda)] - \frac{A_a^{(1)} \gamma_E}{\pi b_0} \ln(1-2\lambda) + \frac{A_a^{(1)} b_1}{2\pi b_0^3} \left[2\lambda + \ln(1-2\lambda) + \frac{1}{2} \ln^2(1-2\lambda) \right] \\ &+ \frac{A_a^{(1)}}{2\pi b_0} [2\lambda + \ln(1-2\lambda)] \ln \frac{Q^2}{\mu_R^2} - \frac{A_a^{(1)}}{\pi b_0} \lambda \ln \frac{Q^2}{\mu_F^2},\end{aligned}\quad (29)$$

$$f_a^{(1)}(\lambda) = -\frac{A_a^{(1)}}{2\pi b_0 \lambda} [(1-2\lambda) \ln(1-2\lambda) - 2(1-\lambda) \ln(1-\lambda)], \quad (30)$$

$$\begin{aligned}
f_a^{(2)}(\lambda, Q^2/\mu_R^2) = & -\frac{A_a^{(1)}b_1}{2\pi b_0^3} \left[\ln(1-2\lambda) - 2\ln(1-\lambda) + \frac{1}{2}\ln^2(1-2\lambda) - \ln^2(1-\lambda) \right] + \frac{B_a^{(1)}}{2\pi b_0} \ln(1-\lambda) \\
& - \frac{A_a^{(1)}\gamma_E}{\pi b_0} [\ln(1-\lambda) - \ln(1-2\lambda)] - \frac{A_a^{(2)}}{2\pi^2 b_0^2} [2\ln(1-\lambda) - \ln(1-2\lambda)] \\
& + \frac{A_a^{(1)}}{2\pi b_0} [2\ln(1-\lambda) - \ln(1-2\lambda)] \ln \frac{Q^2}{\mu_R^2}, \tag{31}
\end{aligned}$$

where b_0, b_1 are the first two coefficients of the QCD β -function:

$$b_0 = \frac{1}{12\pi} (11C_A - 2N_f), \quad b_1 = \frac{1}{24\pi^2} (17C_A^2 - 5C_A N_f - 3C_F N_f). \tag{32}$$

The N -independent coefficients C_{ab} in Eq. (12), which include the hard virtual corrections, have the perturbative expansion

$$C_{ab} = 1 + \frac{\alpha_S}{\pi} C_{ab}^{(1)} + \mathcal{O}(\alpha_S^2). \tag{33}$$

The $C_{ab}^{(1)}$ we need to NLL are obtained by comparing the $\mathcal{O}(\alpha_S)$ -expansion (not counting the overall factor α_S^2 of the Born cross sections) of the resummed expression with the fixed-order NLO result for the process, as given in [19,21]. The full analytic expressions for the $C_{ab}^{(1)}$ are rather lengthy and will not be given here. For convenience, we present them in numerical form in the Appendix. We note that, apart from being useful for extracting the coefficients $C_a^{(1)}$ and $C_{ab}^{(1)}$, the comparison of the $\mathcal{O}(\alpha_S)$ -expanded resummed result with the full NLO cross section also provides an excellent check of the resummation formula, since one can verify that all leading and next-to-leading logarithms are properly accounted for by Eq. (12).

The improved resummed hadronic cross section is finally obtained by performing an inverse Mellin transformation, and by properly matching to the NLO cross section $p_T^3 d\sigma^{(\text{NLO})}(x_T)/dp_T$ as follows:

$$\begin{aligned}
\frac{p_T^3 d\sigma^{(\text{match})}(x_T)}{dp_T} = & \sum_{a,b} \int_{C_{MP}-i\infty}^{C_{MP}+i\infty} \frac{dN}{2\pi i} (x_T^2)^{-N+1} f_{a/H_1}^N(\mu_F^2) \\
& \times f_{b/H_2}^N(\mu_F^2) \\
& \times [\hat{\sigma}_{ab}^{(\text{res})}(N) - (\hat{\sigma}_{ab}^{(\text{res})}(N))_{(\text{NLO})}] \\
& + \frac{p_T^3 d\sigma^{(\text{NLO})}(x_T)}{dp_T}, \tag{34}
\end{aligned}$$

where $\hat{\sigma}_{ab \rightarrow cd}^{(\text{res})}$ is given in Eq. (12) and $(\hat{\sigma}_{ab \rightarrow cd}^{(\text{res})})_{(\text{NLO})}$ represents its perturbative truncation at NLO. Thus, as a result of this matching procedure, in the final cross section in Eq. (34) the NLO cross section is exactly taken into account, and NLL soft-gluon effects are resummed beyond those already contained in the NLO cross section.

The functions $h_a^{(1,2)}(\lambda)$ and $f_a^{(1,2)}(\lambda)$ in Eqs. (28)–(31) are singular at the points $\lambda = 1/2$ and/or $\lambda = 1$. These singularities are related to the divergent behavior of the pertur-

bative running coupling α_S near the Landau pole, and we deal with them by using the *minimal prescription* introduced in Ref. [2]. In the evaluation of the inverse Mellin transformation in Eq. (34), the constant C_{MP} is chosen in such a way that all singularities in the integrand are to the left of the integration contour, except for the Landau singularities, that are taken to lie to its far right. We note that as an alternative to such a definition one could choose to expand the resummed formula to a finite order, say, next-to-next-to-leading order (NNLO), and neglect all terms of yet higher order. This approach was adopted in Ref. [17]. We prefer to keep the full resummed formula in our phenomenological applications since, depending on kinematics, high orders in perturbation theory may still be very relevant [8]. It was actually shown in [2] that the results obtained within the minimal prescription converge asymptotically to the perturbative series.

This completes the presentation of all ingredients to the NLL threshold resummation of the hadronic single-inclusive jet cross section. We will now turn to some phenomenological applications.

IV. PHENOMENOLOGICAL RESULTS

We will study the effects of threshold resummation on the single-inclusive jet cross section in $p\bar{p}$ collisions at $\sqrt{S} = 1.8$ TeV and $\sqrt{S} = 630$ GeV c.m. energies, and in pp collisions at $\sqrt{S} = 200$ GeV. These choices are relevant for comparisons to Tevatron and RHIC data, respectively. Unless otherwise stated, we always set the factorization and renormalization scales to $\mu_F = \mu_R = p_T$ and use the NLO CTEQ6M [31] set of parton distributions, along with the two-loop expression for the strong coupling constant α_S .

We will first analyze the relevance of the different subprocesses contributing to single-jet production. The left part of Fig. 3 shows the relative contributions by “ qq ” ($qq, qq', q\bar{q}$, and $q\bar{q}'$ combined), qg , and gg initial states at Born level (dashed lines) and for the NLL-resummed case (without matching, solid lines). Here we have chosen the case of $p\bar{p}$ collisions at $\sqrt{S} = 1.8$ GeV. As can be seen, the overall change in the curves when going from Born level to

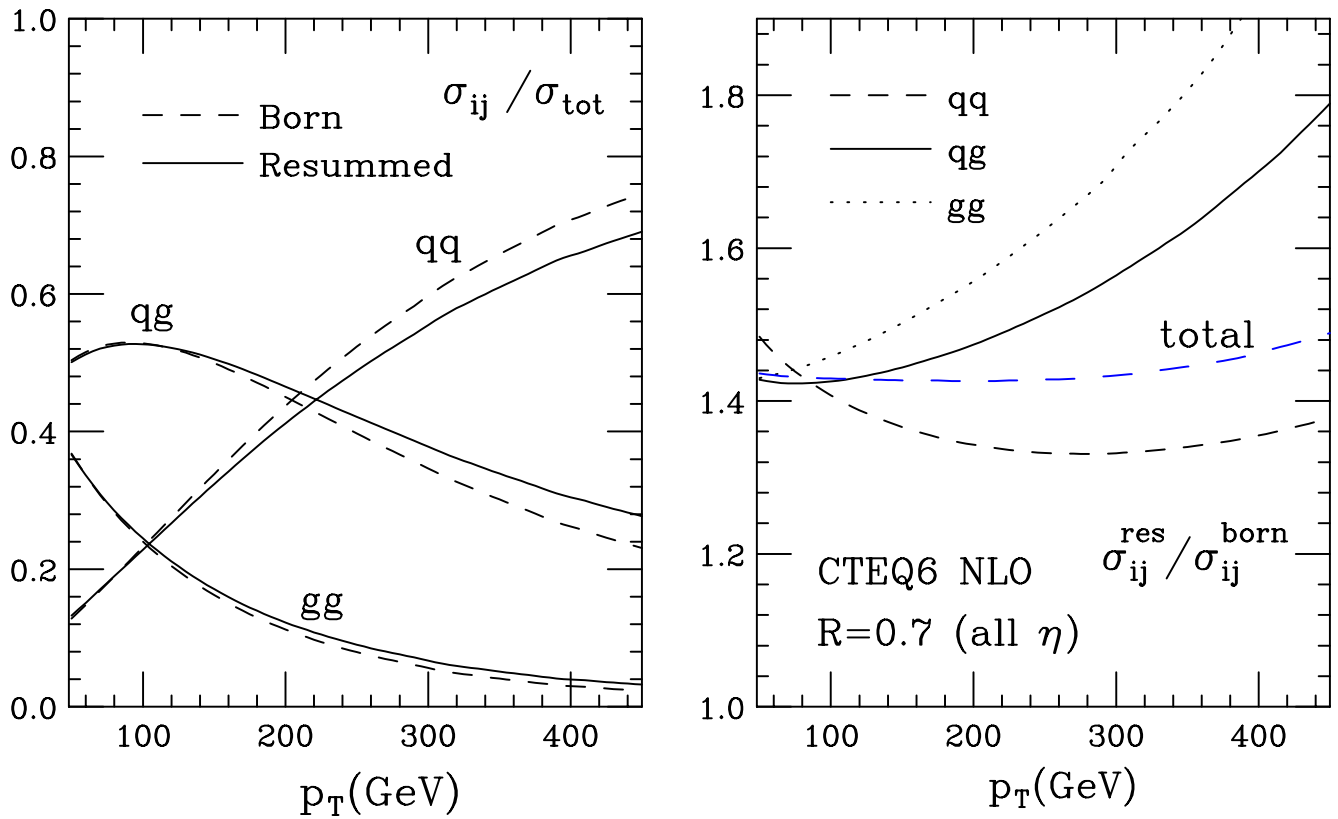


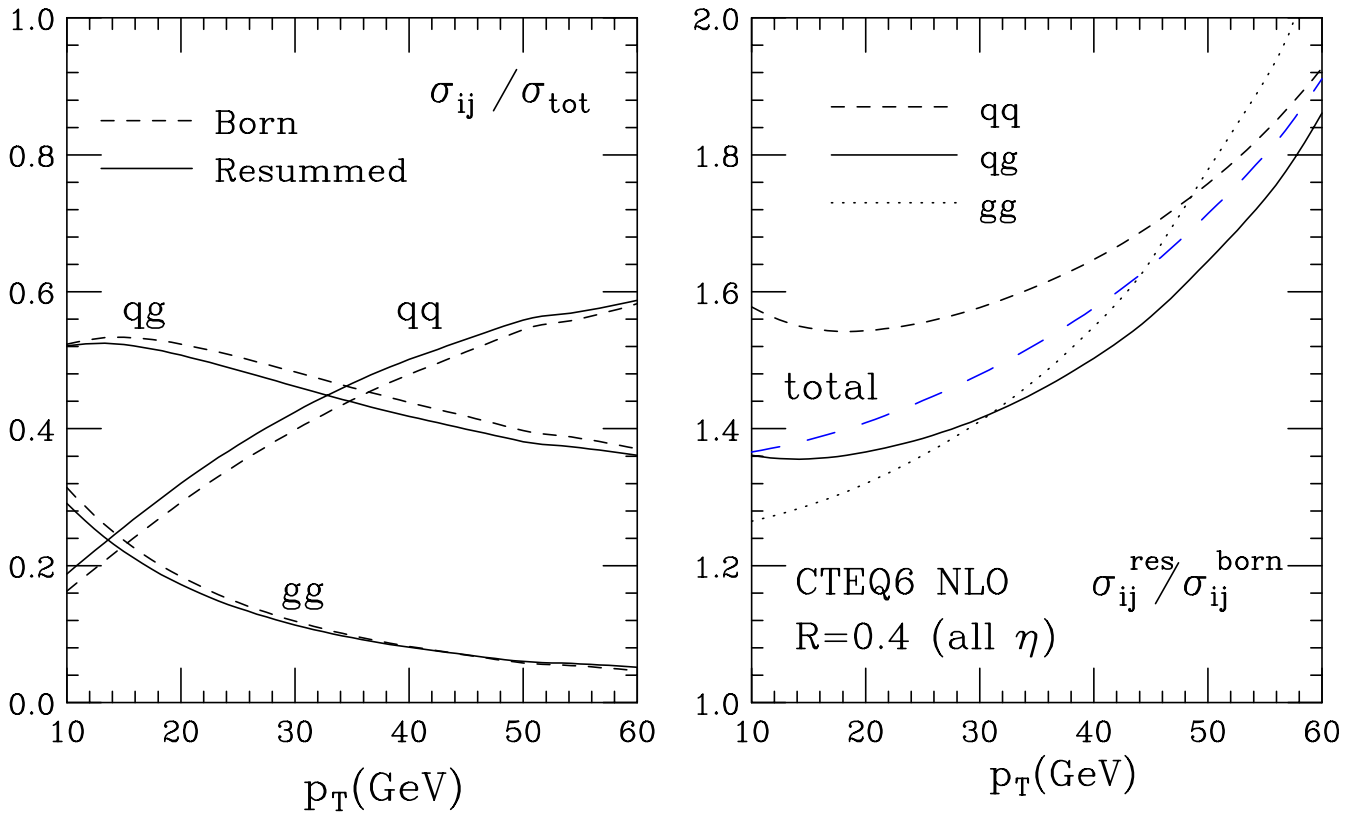
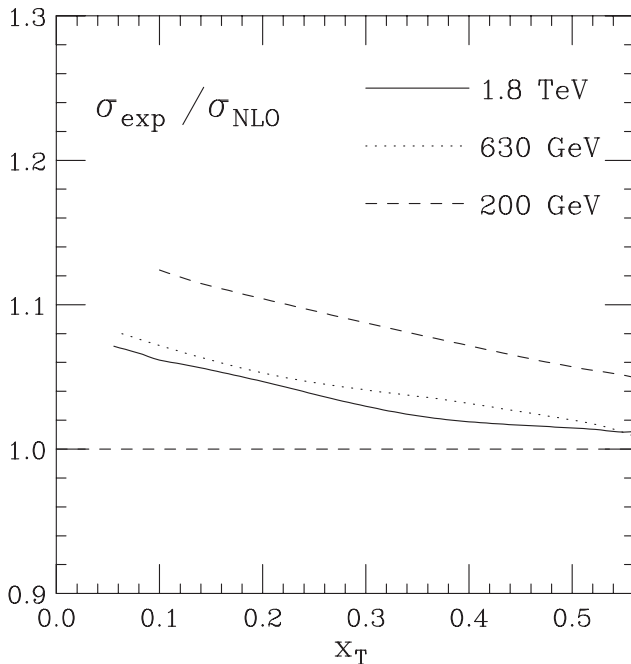
FIG. 3 (color online). Left: relative contributions of the various partonic initial states to the single-inclusive jet cross section in $p\bar{p}$ collisions at $\sqrt{S} = 1.8$ TeV, at Born level (dashed) and for the NLL-resummed case (solid). We have chosen the jet cone size $R = 0.7$. Right: ratios between resummed and Born contributions for the various channels, and for the full jet cross section.

the resummed case is moderate. The main noticeable effect is an increase of the relative importance of processes with gluon initial states toward higher p_T , compensated by a similar decrease in that of the qq channels. In the right part of Fig. 3 we show the enhancements from threshold resummation for each initial partonic state individually, and also for their sum. At the higher p_T , where threshold resummation is expected to be best applicable, the enhancements are biggest for the gg channel, followed by the qg one. All patterns observed in Fig. 3 are straightforwardly understood from Eq. (23), which demonstrates that resummation yields bigger enhancements when the number of gluons in the initial state is larger. We note that results very similar to those shown in the figure hold also at $\sqrt{S} = 630$ GeV, if the same value of $x_T = 2p_T/\sqrt{S}$ is considered. This remains qualitatively true even when we go to pp collisions at $\sqrt{S} = 200$ GeV, except for the larger enhancement in the quark contribution, due to the dominance of the qq channel (instead of the $q\bar{q}$ as in $p\bar{p}$ collisions) with a larger color factor combination in the Sudakov exponent [see the discussion after Eq. (22)].

Figure 4 repeats the studies made for Fig. 3 for this case. As one can see, if the same x_T as in Fig. 3 is considered, the qq scattering contributions are overall slightly less impor-

tant. At the same time, resummation effects are overall somewhat larger because the p_T values are now much smaller than in Fig. 3, so that the strong coupling constant that appears in the resummed exponents is larger.

Before presenting the results for the matched NLL-resummed jet cross section and K -factors, we would like to identify the kinematical region where the logarithmic terms constitute the bulk of the perturbative corrections and subleading contributions are unimportant. Only in these is the resummation expected to provide an accurate picture of the higher-order terms. We can determine this region by comparing the resummed formula, expanded to NLO, to the full fixed-order (NLO) perturbative result, that is, by comparing the last two terms in Eq. (34). Figure 5 shows this comparison for both Tevatron energies and for the RHIC case, as a function of the “scaling” variable x_T . As can be observed, the expansion correctly reproduces the NLO result within at most a few percent over a region corresponding to $p_T \gtrsim 200$ GeV for the higher Tevatron energy, and to $p_T \gtrsim 30$ GeV at RHIC. This demonstrates that, at this order, the perturbative corrections are strongly dominated by the terms of soft and/or collinear origin that are addressed by resummation. The accuracy of the expansion improves toward the larger values of the jet transverse


 FIG. 4 (color online). Same as Fig. 3, but for pp collisions at $\sqrt{s} = 200$ GeV and $R = 0.4$.

 FIG. 5. Ratio between the expansion to NLO of the (unmatched) resummed cross section and the full NLO one (in the SCA), for $p\bar{p}$ collisions at $\sqrt{s} = 1.8$ TeV (solid) and $\sqrt{s} = 630$ GeV (dots), and for pp collisions at $\sqrt{s} = 200$ GeV (dashed).

momentum, where one approaches the threshold limit more closely.

Having established the importance of the threshold corrections in a kinematic regime of interest for phenomenology, we show in Fig. 6 the impact of the resummation on the predicted single-jet cross section at $\sqrt{s} = 1.8$ TeV. NLO and NLL-resummed results are presented, computed at three different values of the factorization and renormalization scales, defined by $\mu_F = \mu_R = \zeta p_T$ (with $\zeta = 1, 2, 1/2$). The most noticeable effect is a remarkable reduction in the scale dependence of the cross section. This observation was also made in the previous study [17]. If, as customary, one defines a theoretical scale “uncertainty” by $\Delta \equiv (\sigma(\zeta = 0.5) - \sigma(\zeta = 2)) / \sigma(\zeta = 1)$, the improvement is considerable. While Δ lies between 20% and 25% at NLO, it never exceeds 8% for the matched NLL result. The inset plot shows the NLL K -factor, defined as

$$K^{(\text{res})} = \frac{d\sigma^{(\text{match})}/dp_T}{d\sigma^{(\text{NLO})}/dp_T}, \quad (35)$$

at each of the scales. The corrections from resummation on top of NLO are typically very moderate, at the order of a few percent, depending on the set of scales chosen. The higher-order corrections increase for larger values of the jet transverse momentum. These findings are again consistent

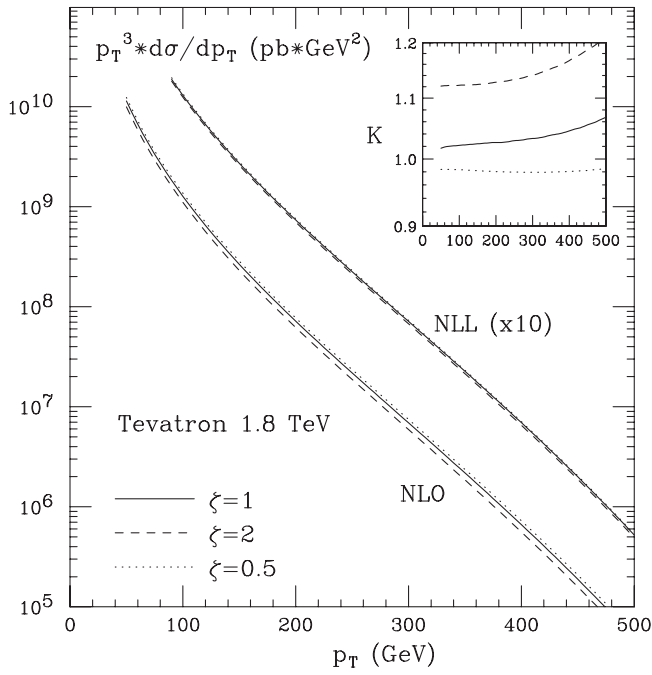


FIG. 6. NLO and NLL results for the single-inclusive jet cross section in $p\bar{p}$ collisions at $\sqrt{s} = 1.8$ TeV, for different values of the renormalization and factorization scales. We have chosen $R = 0.7$. The inset plot shows the corresponding K -factors as defined in Eq. (35).

with those of [17], even though more detailed comparisons reveal some quantitative differences that must be related to either the different choice of the resummed final-state jet function in [17] (see discussion in Sec. III), or to the fact that [17] uses only a NNLO expansion of the resummed cross section. The main features of our results remain unchanged when we go to the Tevatron-run II energy of $\sqrt{s} = 1.96$ TeV, at which measured jet cross sections are now available [37]. Quantitatively very similar results are also found for the lower Tevatron center-of-mass energy, as seen in Fig. 7. In the case of pp collisions at $\sqrt{s} = 200$ GeV, presented in Fig. 8, a similar pattern emerges, even though the resummation effects tend to be overall somewhat more substantial here.

In Fig. 9 we analyze how the resummation effects build up order by order in perturbation theory. We expand the matched resummed formula beyond NLO and define the “partial” soft-gluon K -factors as

$$K^n \equiv \frac{d\sigma^{(\text{match})}/dp_T|_{\mathcal{O}(\alpha_s^{2+n})}}{d\sigma^{(\text{NLO})}/dp_T}, \quad (36)$$

which for $n = 2, 3, \dots$ give the additional enhancement over full NLO due to the $\mathcal{O}(\alpha_s^{2+n})$ terms in the resummed formula.⁵ Formally, $K^1 = 1$ and $K^\infty = K^{(\text{res})}$ of Eq. (35).

⁵We recall that the Born cross sections are of $\mathcal{O}(\alpha_s^2)$, hence the additional power of 2 in this definition.

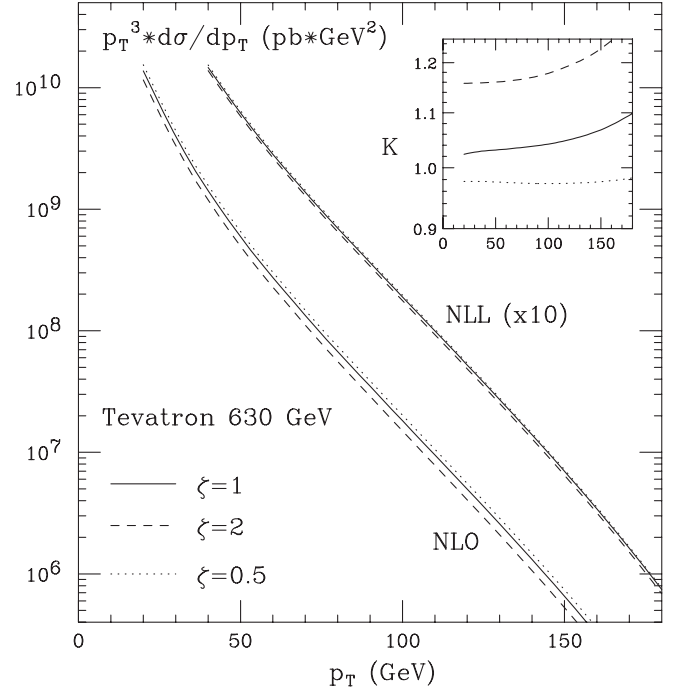


FIG. 7. Same as Fig. 6, but for $\sqrt{s} = 630$ GeV.

The results for $K^{2,3,4,\infty}$ are given in the figure, for the case of $p\bar{p}$ collisions at $\sqrt{s} = 1.8$ TeV. One can see that contributions beyond $N^3\text{LO}$ ($n = 3$) are very small, and that the $\mathcal{O}(\alpha_s^6)$ result can hardly be distinguished from the full NLL one.

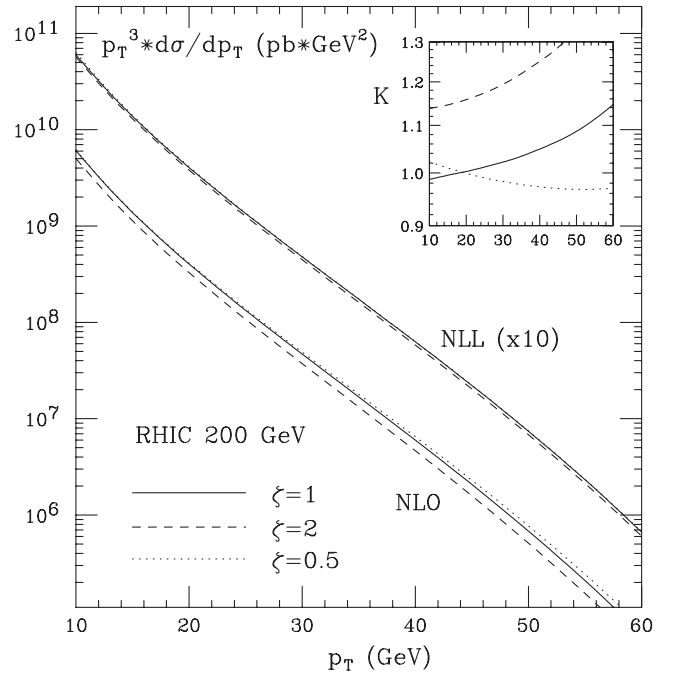


FIG. 8. Same as Fig. 6, but for pp collisions at $\sqrt{s} = 200$ GeV and $R = 0.4$.

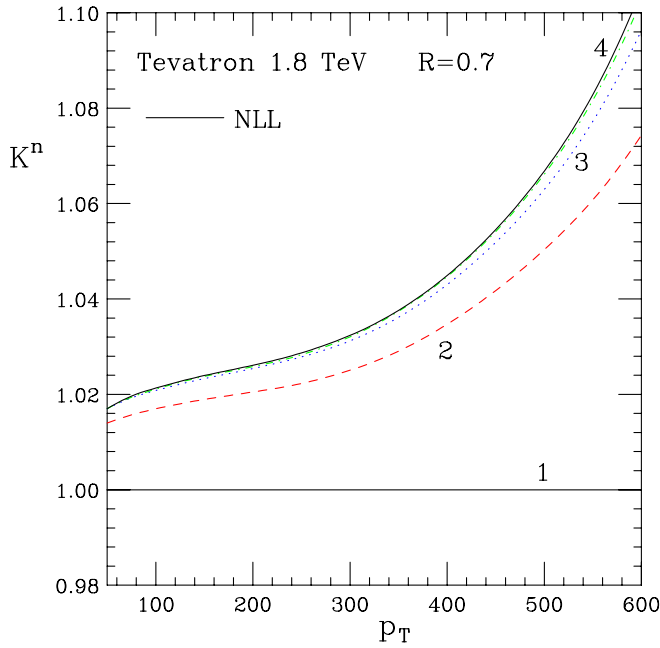


FIG. 9 (color online). Soft-gluon K^n factors as defined in Eq. (36), for $p\bar{p}$ collisions at $\sqrt{S} = 1.8$ TeV.

It is interesting to contrast the rather modest enhancement of the jet cross section by resummation to the dramatic resummation effects that we observed in [8] in the case of single-inclusive pion production, $H_1 H_2 \rightarrow \pi X$, in

fixed-target scattering at typical c.m. energies of $\sqrt{S} \sim 30$ GeV. Even though in both cases the same partonic processes are involved at the Born level, there are several important differences. First of all, the values of p_T are much smaller in fixed-target scattering (even though roughly similar values of $x_T = 2p_T/\sqrt{S}$ are probed), so that the strong coupling constant $\alpha_S(p_T)$ is larger and resummation effects are bound to be more significant. Furthermore, for the process $H_1 H_2 \rightarrow \pi X$, one needs to introduce fragmentation functions into the theoretical calculation that describes the formation of the observed hadron from a final-state parton. As the hadron takes only a certain fraction $z \geq 0.5$ of the parent parton's momentum, the partonic hard-scattering necessarily has to be at the higher transverse momentum p_T/z in order to produce a hadron with p_T . Thus, one is closer to partonic threshold than in the case of a jet produced with transverse momentum p_T which takes *all* of a final-state parton's momentum. In addition, it turns out [8,38] that, due to the factorization of final-state collinear singularities associated with the fragmentation functions, the jet function J_N^c in the resummation formula [Eq. (12)] is to be replaced by a factor Δ_N^c , which has enhancing double logarithms.

Finally, as one illustrative example, we compare our resummed jet cross section to data from CDF [13] at $\sqrt{S} = 1800$ GeV. While so far we have always considered the cross section integrated over all jet rapidities, we here need

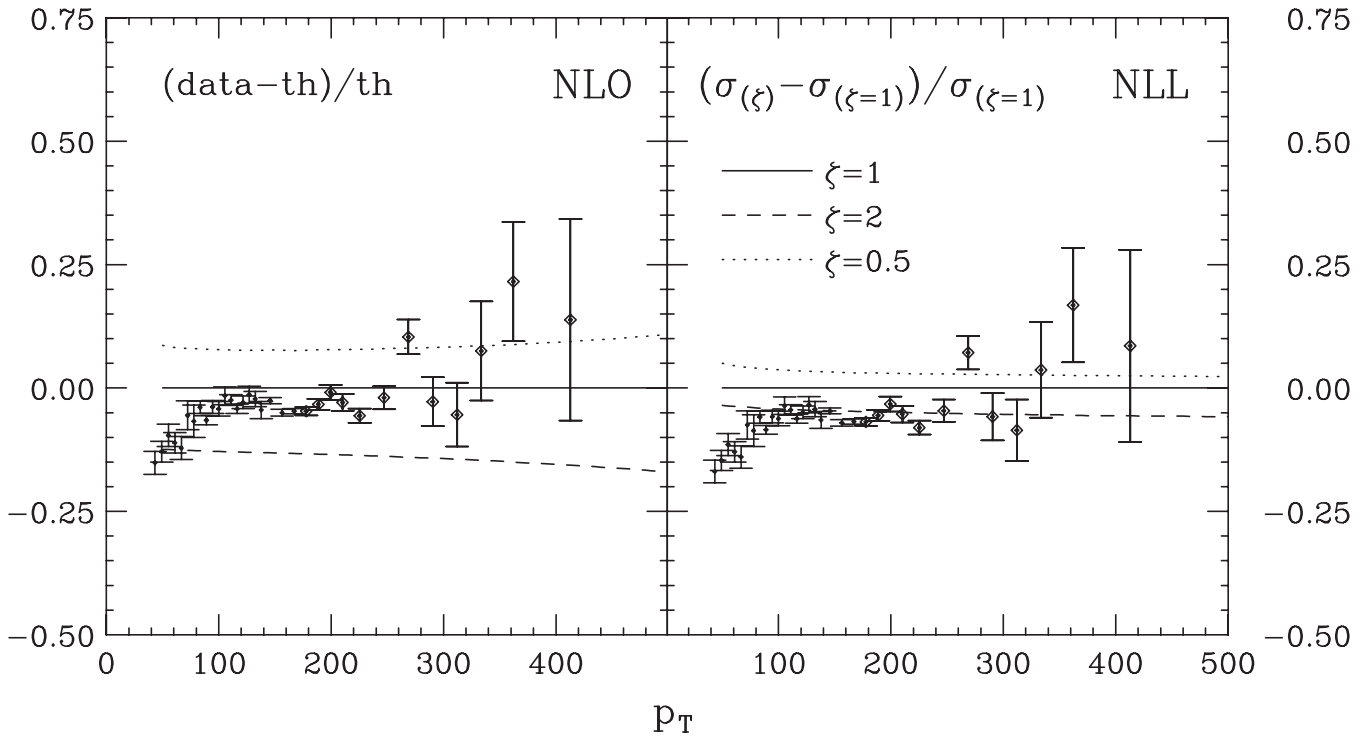


FIG. 10. Ratios “(data-theory)/theory” for data from CDF at 1.8 TeV [13] and for NLO and NLL-resummed theoretical calculations. We have chosen the theory result at scale p_T as “default”; results for other scales are also displayed in terms of their relative shifts with respect to the default theory.

to account for the fact that the data cover only a finite region in rapidity, $0.1 \leq |\eta| \leq 0.7$. Also, we would like to properly match the jet algorithm chosen in experiment, rather than using the SCA. We have mentioned before that both these issues can be accurately addressed by “rescaling” the resummed cross section by an appropriate ratio of NLO cross sections. We simply multiply our K -factors defined in Eq. (35) and shown in Fig. 6 by $d\sigma^{(\text{MC})}(0.1 \leq |\eta| \leq 0.7)/dp_T$, the NLO cross section obtained with a full Monte Carlo code [24], in the experimentally accessed rapidity regime. The comparison between the data and the NLO and NLL-resummed cross sections is shown in Fig. 10 in terms of the ratios “(data – theory)/theory.” As expected from Fig. 6, the impact of resummation is moderate and in fact smaller than the current uncertainties of the parton distributions [37]. Nonetheless, it does lead to a slight improvement of the comparison and, in particular, the plot again demonstrates the reduction of scale dependence by resummation.

V. CONCLUSIONS

We have studied in this paper the resummation of large logarithmic threshold corrections to the partonic cross sections contributing to single-inclusive jet production at hadron colliders. Our study differs from previous work [17] mostly in that we allow the jet to have a finite invariant mass at partonic threshold, which is consistent with the experimental definitions of jet cross sections and with the available NLO calculations. Moreover, using semianalytical expressions for the NLO partonic cross sections derived in the SCA [19,21], we have extracted the N -independent coefficients that appear in the resummation formula, and properly matched our resummed cross section to the NLO one. We hope that with these improvements yet more realistic estimates of the higher-order corrections to jet cross sections in the threshold regime emerge.

It is well known that the NLO description of jet production at hadron colliders is overall very successful, within the uncertainties of the theoretical framework and the experimental data. From that perspective, it is gratifying to see that the effects of NLL resummation are relatively moderate. On the other hand, resummation leads to a significant decrease of the scale dependence, and we expect that knowledge of the resummation effects should be useful in comparisons with future, yet more precise, data, and for extracting parton distribution functions. Given the

general success of the NLO description, we have mostly focused on K -factors for the resummed cross section over the NLO one, and only given one example of a more detailed comparison with experimental data. We believe that these K -factors may be readily used in conjunction with other, more flexible NLO Monte Carlo programs for jet production, to estimate threshold-resummation effects on cross sections for other jet algorithms and possibly for larger cone sizes.

ACKNOWLEDGMENTS

We are grateful to Stefano Catani, Barbara Jäger, Nikolaos Kidonakis, Douglas Ross, George Sterman, and Marco Stratmann for helpful discussions. D. d. F. is supported in part by UBACYT and CONICET. W. V. is supported by the U.S. Department of Energy under Contract No. DE-AC02-98CH10886.

APPENDIX: FIRST-ORDER COEFFICIENTS $C_{ab}^{(1)}$ IN THE SCA

In this Appendix we collect the process-dependent coefficients $C_{ab}^{(1)}$ for the various partonic channels in jet hadroproduction in the SCA. The $C_{ab}^{(1)}$ are constant, that is, they do not depend on the Mellin-moment variable N . They may be extracted by expanding the resummed cross section in Eq. (12) to first order and comparing it to the full NLO cross section in the SCA. For the sake of simplicity, we provide the $C_{ab}^{(1)}$ only in numerical form, as the full analytic coefficients have relatively lengthy expressions. We find

$$\begin{aligned}
 C_{qq'}^{(1)} &= 17.9012 + 1.387\,63 \log \frac{R}{2}, \\
 C_{q\bar{q}'}^{(1)} &= 19.0395 + 1.387\,63 \log \frac{R}{2}, \\
 C_{q\bar{q}}^{(1)} &= 13.4171 + 1.6989 \log \frac{R}{2}, \\
 C_{qq}^{(1)} &= 17.1973 + 1.387\,63 \log \frac{R}{2}, \\
 C_{qg}^{(1)} &= 14.4483 + 2.588\,24 \log \frac{R}{2}, \\
 C_{gg}^{(1)} &= 14.5629 + 3.678\,84 \log \frac{R}{2},
 \end{aligned} \tag{A1}$$

where R is the jet cone size.

-
- [1] G. Sterman, Nucl. Phys. **B281**, 310 (1987); S. Catani and L. Trentadue, Nucl. Phys. **B327**, 323 (1989); **B353**, 183 (1991).
 [2] S. Catani, M.L. Mangano, P. Nason, and L. Trentadue,

- Nucl. Phys. **B478**, 273 (1996).
 [3] N. Kidonakis and G. Sterman, Nucl. Phys. **B505**, 321 (1997).
 [4] N. Kidonakis, G. Oderda, and G. Sterman, Nucl. Phys.

- B525**, 299 (1998).
- [5] N. Kidonakis, G. Oderda, and G. Sterman, Nucl. Phys. **B531**, 365 (1998).
- [6] E. Laenen, G. Oderda, and G. Sterman, Phys. Lett. B **438**, 173 (1998).
- [7] R. Bonciani, S. Catani, M.L. Mangano, and P. Nason, Phys. Lett. B **575**, 268 (2003).
- [8] D. de Florian and W. Vogelsang, Phys. Rev. D **71**, 114004 (2005).
- [9] S. Catani, M.L. Mangano, and P. Nason, J. High Energy Phys. 07 (1998) 024; S. Catani, M.L. Mangano, P. Nason, C. Oleari, and W. Vogelsang, J. High Energy Phys. 03 (1999) 025.
- [10] N. Kidonakis and J.F. Owens, Phys. Rev. D **61**, 094004 (2000).
- [11] G. Sterman and W. Vogelsang, J. High Energy Phys. 02 (2001) 016.
- [12] D. de Florian and W. Vogelsang, Phys. Rev. D **72**, 014014 (2005).
- [13] A. A. Affolder *et al.* (CDF Collaboration), Phys. Rev. D **64**, 032001 (2001); **65**, 039903(E) (2002).
- [14] B. Abbott *et al.* (D0 Collaboration), Phys. Rev. Lett. **82**, 2451 (1999); Phys. Rev. D **64**, 032003 (2001); V.M. Abazov *et al.* (D0 Collaboration), Phys. Lett. B **525**, 211 (2002).
- [15] S. Kuhlmann, H.L. Lai, and W.K. Tung, Phys. Lett. B **409**, 271 (1997); J. Huston *et al.*, Phys. Rev. Lett. **77**, 444 (1996); H.L. Lai *et al.*, Phys. Rev. D **55**, 1280 (1997).
- [16] B.I. Abelev *et al.* (STAR Collaboration), Phys. Rev. Lett. **97**, 252001 (2006).
- [17] N. Kidonakis and J.F. Owens, Phys. Rev. D **63**, 054019 (2001).
- [18] For initial work on jet production in the “soft-collinear effective theory,” see C.W. Bauer and M.D. Schwartz, Phys. Rev. Lett. **97**, 142001 (2006).
- [19] M. Furman, Nucl. Phys. **B197**, 413 (1982); F. Aversa, P. Chiappetta, M. Greco, and J.P. Guillet, Nucl. Phys. **B327**, 105 (1989); Z. Phys. C **46**, 253 (1990).
- [20] J.P. Guillet, Z. Phys. C **51**, 587 (1991).
- [21] B. Jäger, M. Stratmann, and W. Vogelsang, Phys. Rev. D **70**, 034010 (2004).
- [22] See also S.G. Salesch, Ph.D. thesis, Hamburg University [DESY-93-196, 1993 (unpublished)].
- [23] F. Aversa, P. Chiappetta, M. Greco, and J.-Ph. Guillet, Phys. Rev. Lett. **65**, 401 (1990); F. Aversa, P. Chiappetta, L. Gonzales, M. Greco, and J.-Ph. Guillet, Z. Phys. C **49**, 459 (1991).
- [24] S. Frixione, Nucl. Phys. **B507**, 295 (1997); D. de Florian, S. Frixione, A. Signer, and W. Vogelsang, Nucl. Phys. **B539**, 455 (1999).
- [25] J.E. Huth *et al.*, FERMILAB-CONF-90-249-E, 1990.
- [26] S.D. Ellis, Z. Kunszt, and D.E. Soper, Phys. Rev. Lett. **62**, 726 (1989); Phys. Rev. D **40**, 2188 (1989); Phys. Rev. Lett. **64**, 2121 (1990); **69**, 3615 (1992).
- [27] J. Alitti *et al.* (UA2 Collaboration), Phys. Lett. B **257**, 232 (1991); F. Abe *et al.* (CDF Collaboration), Phys. Rev. D **45**, 1448 (1992); S. Abachi *et al.* (D0 Collaboration), Phys. Rev. D **53**, 6000 (1996).
- [28] S. Catani, Yu.L. Dokshitzer, M.H. Seymour, and B.R. Webber, Nucl. Phys. **B406**, 187 (1993); S.D. Ellis and D.E. Soper, Phys. Rev. D **48**, 3160 (1993).
- [29] See also the discussions about jet definitions and algorithms in, for example, W.B. Kilgore and W.T. Giele, Phys. Rev. D **55**, 7183 (1997); M.H. Seymour, Nucl. Phys. **B513**, 269 (1998); *Proceedings of the “8th International Workshop on Deep Inelastic Scattering and QCD (DIS 2000),” Liverpool, England, 2000*, edited by J.A. Gracey and T. Greenshaw (World Scientific, Singapore, 2001), p. 27.
- [30] See J.C. Collins, D.E. Soper, and G. Sterman, Adv. Ser. Dir. High Energy Phys. **5**, 1 (1988), and references therein.
- [31] J. Pumplin *et al.*, J. High Energy Phys. 07 (2002) 012.
- [32] J. Kodaira and L. Trentadue, Phys. Lett. **112B**, 66 (1982); **123B**, 335 (1983); S. Catani, E. D’Emilio, and L. Trentadue, Phys. Lett. B **211**, 335 (1988).
- [33] N. Kidonakis, Int. J. Mod. Phys. A **15**, 1245 (2000).
- [34] The two-loop corrections to these anomalous dimension matrices were recently calculated in S. Mert Aybat, L.J. Dixon, and G. Sterman, Phys. Rev. Lett. **97**, 072001 (2006); Phys. Rev. D **74**, 074004 (2006).
- [35] M. Dasgupta and G.P. Salam, Phys. Lett. B **512**, 323 (2001); J. High Energy Phys. 03 (2002) 017.
- [36] C.F. Berger, T. Kucs, and G. Sterman, Phys. Rev. D **65**, 094031 (2002).
- [37] A. Abulencia (CDF Run II Collaboration), Phys. Rev. D **75** 092006 (2007); **75** 119901 (2007); M. Voutilainen (D0 Collaboration), arXiv:hep-ex/0609026.
- [38] M. Cacciari and S. Catani, Nucl. Phys. **B617**, 253 (2001).